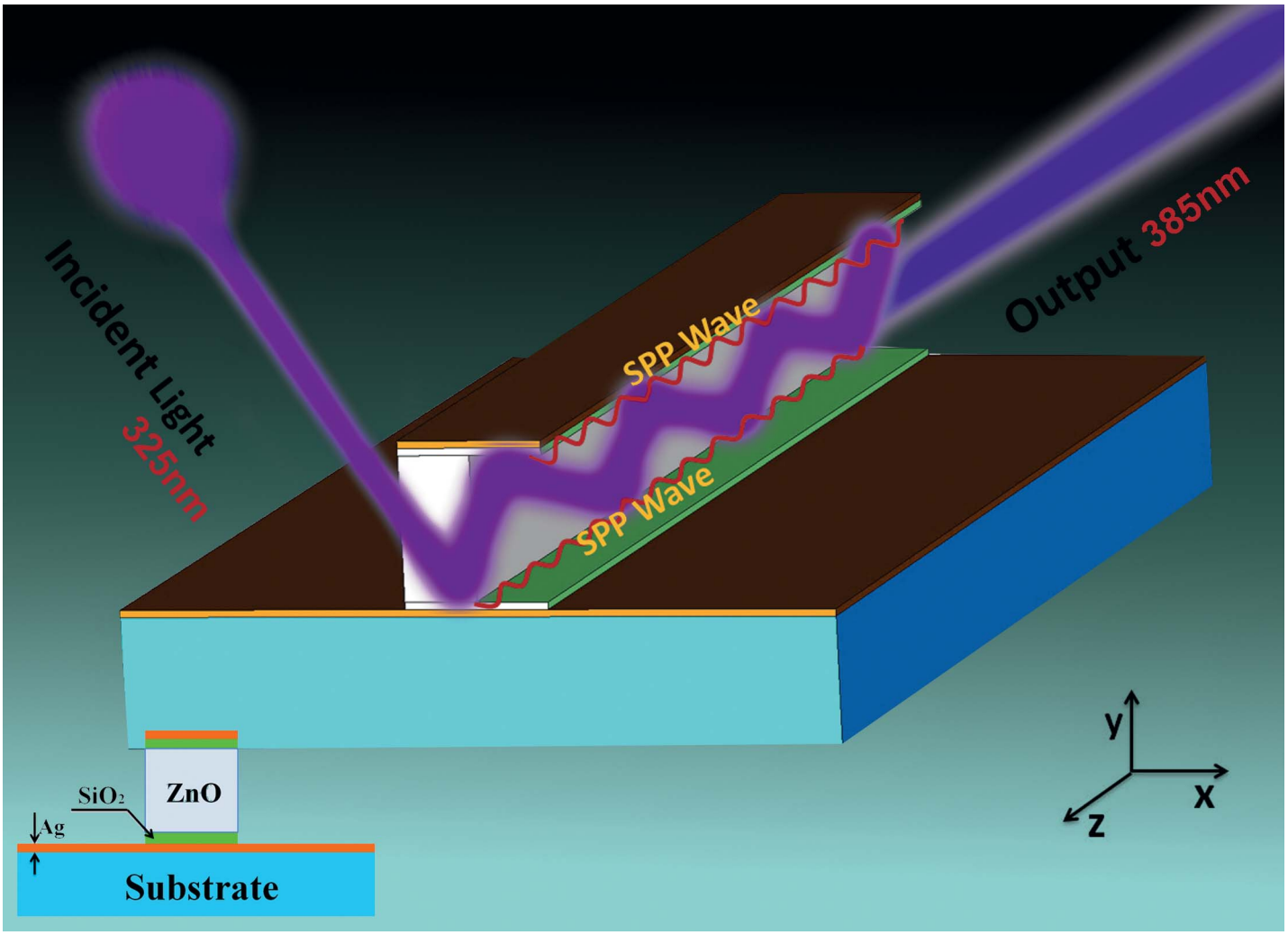

Showcasing research from the State key Laboratory of Luminescence and Applications, Changchun Institute of Optics, Fine Mechanics and Physics, Chinese Academy of Sciences.

Title: Plasmon-enhanced ultraviolet photoluminescence from the hybrid plasmonic Fabry–Perot microcavity of Ag/ZnO microwire

A type of hybrid plasmonic Fabry–Perot (F–P) microcavity consisting of ZnO microwire with quadrate cross section and plasmonic MIM homo-waveguides with a nanoscale SiO_2 gap between has been constructed. This type of microcavity structure can support subwavelength confinement and long range propagation. Compared with bare ZnO microwire, two orders of magnitude enhancement of the photoluminescence intensity has been achieved.

As featured in:

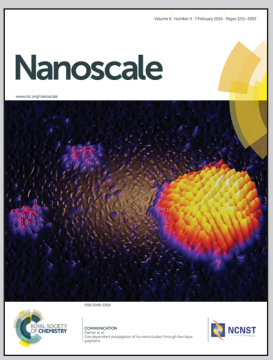

See Zhao *et al.*, *Nanoscale*, 2014, **6**, 1354.

ROYAL SOCIETY OF CHEMISTRY

www.rsc.org/nanoscale

Registered charity number: 207890

Nanoscale

PAPER

View Article Online
View Journal | View Issue

Plasmon-enhanced ultraviolet photoluminescence from the hybrid plasmonic Fabry–Perot microcavity of Ag/ZnO microwires

Cite this: *Nanoscale*, 2014, **6**, 1354

Ming-Ming Jiang,[a] Bin Zhao,[ab] Hong-Yu Chen,[ab] Dong-Xu Zhao,*[a] Chong-Xin Shan[a] and De-Zhen Shen*[a]

Received 27th September 2013
Accepted 4th November 2013

DOI: 10.1039/c3nr05119f

www.rsc.org/nanoscale

We propose a kind of hybrid plasmonic Fabry–Perot (F–P) microcavity consisting of ZnO microwires with quadrate cross-section and planar multilayer metal–insulator–metal (MIM) homostructures with a nanoscale SiO_2 gap in between. MIM homostructures can be used to create a micro-resonator that simultaneously provides feedback for laser action and supports the coupling between the plasmonic waveguide modes and microwire modes across the gap. The hybridization of ZnO microwire modes and surface plasmons across the gap forms hybrid plasmonic F–P microcavity modes, which are highly confined to the low-loss SiO_2 gap region. By comparing with bare ZnO microwires, an enhancement in photoluminescence (PL) intensity of two orders of magnitude is realized experimentally due to the coupling between plasmonic MIM homostructures and ZnO microwires. The controllability and miniaturization emission properties of this type of microcavity are potentially important for designing laser cavity applications and information transmission.

1. Introduction

Remarkable devices based on optical microcavities are already indispensable for a wide range of applications and studies because of their geometrical and resonant properties.[1–5] Taking active wide bandgap semiconductor materials for example, microcavities can be used to control laser emission spectra to enable long-distance transmission of data over optical fibres. Semiconductor nanowire (NW) and microwire (MW) cavities with tailorable optical modes have been used to develop nanoscale oscillators and amplifiers in lasers,[6] sensors,[7] and single photon emitters.[8] An ideal cavity would confine light indefinitely (that is, without loss) and would have resonant frequencies at precise values.[1] The lasing actions of the semiconductor nano/micro-structures have been reported as random type,[9,10] Fabry–Perot (F–P) type,[11,12] and whispering gallery mode (WGM) type lasing,[13] each with distinctly different resonant cavity structures.

Lower cost, higher power and shorter wavelengths of ultraviolet semiconductor lasers have motivated interest in zinc oxide (ZnO) due to its wide direct bandgap and a large exciton binding energy. While possessing natural resonant cavities, ZnO nanowires and microwires are an ideal platform to realize laser diodes, efficient light emitting devices (LED) and so on.[14–17] Aiming at creating enhanced luminescence emission from ZnO nanostructures, much attention has been paid to the resonant cavity devices with the F–P and the WGM modes based on ZnO microstructures and nanostructures, such as microwires, microdisks, and nanonails. Optimization of experimental conditions can yield moderate control over the structure diameter.[6,11–13] High quality quadrilateral ZnO microwires have been prepared, and the corresponding laser action is also achieved. ZnO microwires with quadrate cross-section exhibit a low threshold excitation intensity of 58 kW cm^{-2} and a quality factor of 485.[12] The F–P type laser action was observed in quadrilateral ZnO microwires, where the top and bottom facets of the cross-section served as two reflecting mirrors. Especially, the quadrilateral ZnO microwire is a natural microcavity for lasing with a low lasing threshold, distinct lasing modes, and definite lasing output directions. A high-performance F–P cavity would own resonance modes at precise values and confine light with low loss which can be described by the cavity quality factor Q. Upon comparison with the results of the WGM microcavity and NW nanocavity, the Q-factor is much lower.[6,13] Therefore, it is essential for us to develop new methods to improve resonance modes and enhance the Q-factor of the F–P microcavity.[18,19]

Surface plasmon polaritons (SPPs), which are electromagnetic waves coupled with the oscillation of collective electrons bound to a metal–dielectric interface, afforded to be a promising route for advances in SPP amplification and lasing.[20] Convincing demonstrations of SPP amplification and lasing

[a]*State Key Laboratory of Luminescence and Applications, Changchun Institute of Optics, Fine Mechanics and Physics, Chinese Academy of Sciences, Dongnanhu Road 3888, Changchun, 130033, People's Republic of China. E-mail: zhaodx@ciomp.ac.cn; shendz@ciomp.ac.cn*

[b]*University of the Chinese Academy of Sciences, Beijing, 100049, People's Republic of China*

have been reported in various systems involving single-interface, long-range, short-range and resonant SPPs. Studies of plasmonic cavities with nanoscale dimensions are currently a popular research topic.[21–23] Metal coated semiconductor quantum dots, semiconductor nanowires and microwires have been studied and applied to physical, chemical, and biological sciences.[24,25] Much work on the development of new types of nano/micro-cavity structures composed of metal-cladded waveguides and other planar structures remains, particularly for applications that demand high performance and usability.[26–29]

There are few investigations that have been reported on metal cladded F–P and WGM cavities, which can be used to improve the performance of devices based on an individual microstructure and nanostructure.[30,31] In this contribution, a hybrid optical F–P microcavity consisting of quadrilateral ZnO microwires and MIM homostructures was proposed. ZnO microwires served as the intrinsic F–P cavity coupled to the metal layers with a nanoscale SiO_2 gap.[32,33] Using coupled-mode theory, the mode characteristics of the hybrid plasmonic F–P microcavity have been demonstrated.[34,35] Experimentally, ZnO microwires were synthesized, and ultraviolet PL intensities of the hybrid plasmonic F–P microcavity were systemically investigated. Two orders of magnitude of PL enhancement have been achieved. In order to confirm the enhancement derived from the hybrid plasmonic F–P microcavity, hybrid plasmonic waveguides consisting of double gold films or a single silver film based on MIM homostructures and ZnO microwires with quadrate cross-section were also proposed, but few enhancement phenomena were observed.

2. Mode characteristics of the hybrid plasmonic Fabry–Perot microcavity

A hybrid plasmonic F–P microcavity based on the quadrilateral ZnO microwire was built; the geometry of the studied system is shown in Fig. 1. The quadrilateral ZnO microwire is a natural F–P microcavity, the top and bottom metal layers together with the dielectric layers form another F–P microcavity. This microcavity can be viewed as built based on the hybrid plasmonic waveguide, where SPPs provided a new way to confine electromagnetic (EM) waves beyond the diffraction limit by storing the optical energy in free electron oscillations along the metal–dielectric interface.[28,30,36] Facets of the microwires served as two reflecting mirrors. In order to adjust the mode characteristics of the hybrid plasmonic F–P microcavity and to reduce the loss of metal, SiO_2 as the filler was used in the contact region between silver films and ZnO microwires. This is known as *spaser*, which can be used to compensate loss by optical gain in localized and propagating surface plasmons and even allowed the amplification of propagating surface plasmons.[37,38] Cavities are fascinating tools to enhance light–matter interactions within the framework of cavity quantum electrodynamics. When a single emitter was placed in a cavity, it is demonstrated that the spontaneous emission rate can be greatly modified due to the Purcell effect and even vacuum Rabi splitting can be achieved.[28,30,32] The hybrid plasmonic F–P microcavity generally admitted that the extraordinary transmission is mainly derived from the excitation of coupled surface plasmons on the upper and lower interfaces of the metal films for two-dimensional and one-dimensional structures, where a strong coupling interaction between localized plasmons and propagating plasmons can be achieved, and a strong field enhancement can also be achieved due to efficient coupling of the microwire mode and the cavity mode as shown in Fig. 2.[26,33] Fig. 2 demonstrates that when light is incident on the ZnO microwire, as for the top and bottom reflection mirrors, the light will oscillate back and forth along the axis of the ZnO microwire. The surface plasmon wave was excited when photons were incident to the interface of silver films and the SiO_2 thin film and would propagate along the axis. Here, the interaction of a ZnO microwire with a metallic plasmonic Fabry–Perot cavity was investigated. Compared with previous studies, we paid attention to emphasizing the importance of the mode characteristics of the plasmonic microcavity, which is referred to as the F–P cavity confining the propagating plasmon at the SiO_2–metal interface between the two mirrors. Unlike the photonic cavity, where the

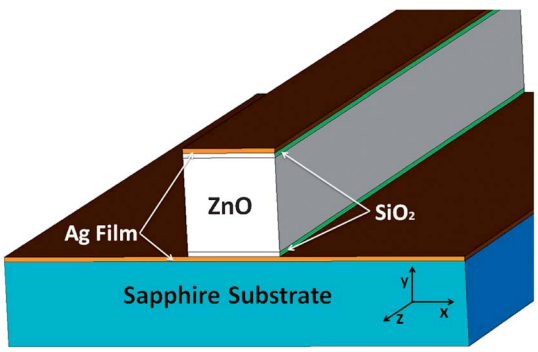

Fig. 1 Schematic diagram of the hybrid plasmonic F–P microcavity: the MIM homostructure is placed on the substrate; a quadrilateral ZnO microwire placed between two Ag layers, whilst a small SiO_2 gap.

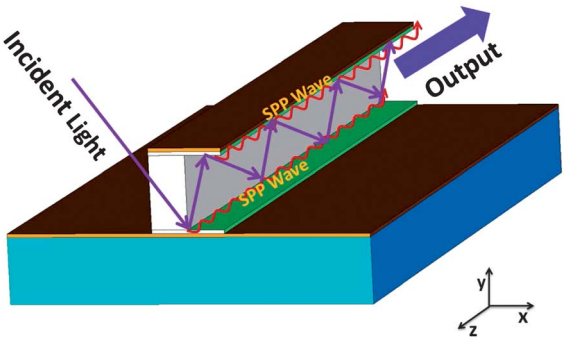

Fig. 2 Schemes of the hybrid plasmonic F–P microcavity: during the optical excitation to the cross-section of the microcavity, light can spread along the z-axis, whilst the light into the interface of SiO_2 and metal films, surface plasmon oscillation, can be excited, so that the surface plasmon wave can also be propagated along the z-axis at the interface. The metal layer is silver with a permittivity of $\varepsilon_{Ag} = -129 + 3.3i$, $\varepsilon_{ZnO} = 4.5$, and $\varepsilon_{SiO2} = 2.25$ at the telecommunications wavelength $\lambda_i = 1550$ nm. The centre of the ZnO microwire defines the origin ($x = y = 0$).

ultimate mode volume of the photonic mode is diffraction limited, the surface plasmon mode is tightly confined at the metal–dielectric interface and the electromagnetic field is strongly enhanced in the hybrid plasmonic F–P microcavity.[21,34]

Using coupled-mode theory, the hybrid mode as a superposition of the microwire modes (without the double metallic film region) and the SPP waveguide modes was described (without the microwire).[26] Fig. 3(a)–(c) show the normalized energy density **W**, the electromagnetic field **E**(**x**, **y**) and $\mathbf{E}_y$ distributions for the hybrid plasmonic mode with TM polarization (where the electric field is perpendicular to the surface of the substrate) for the top and bottom SiO_2 gap layers. The mode characteristics of the hybrid plasmonic F–P microcavity were studied with the variables of the width of the quadrilateral ZnO microwire defined as d and the gap distance between metal films and ZnO microwires defined as g. For large d and small g values (for example, $[d, g] = [3, 0.005]$ μm), the hybrid plasmonic waveguide supports a low-loss cylinder photonic-like mode with optical energy confined to the dielectric waveguide core. The microwire mode is strongly coupled with the SPP mode, and partial optical energy is concentrated inside the SiO_2 gap with an ultrasmall mode area as shown in Fig. 3(a)–(c).

In order to further understand the hybrid plasmonic F–P microcavity, a three-dimensional space simulation based on the model was studied as shown in Fig. 3. The surface plasmon wave excited at the interface between metal films and low dielectric film layers can be transmitted along the interface with very low energy loss. Furthermore, along the y–z plane, when the excitation light source struck the quadrate cross-section of the microwire, light may be transmitted along the z-axial vibration as shown in Fig. 3(e). As is well known that the oscillation pattern of the F–P cavity is relatively single, energy can oscillate back and forth inside the cavity and spread along the axis of the microwire.

Fig. 4 demonstrates the distribution of energy density **W**, electric field **E**(**x**, **y**) and the y component of the electric field $\mathbf{E}_y$ of the ZnO microwire with quadrate cross-section of the hybrid plasmonic F–P microcavity. Fig. 4(a) and (d) show that the electromagnetic energy density is mainly concentrated in the ZnO microwire; therefore, energy was transmitted along the axis of the microwire. Fig. 4(b) and (e) demonstrate the distribution of the electric field **E**(**x**, **y**) along $x = 0$, and show the confinement in the low-index dielectric region. For an ultrasmall low dielectric layer as filler, the hybrid waveguide supports a low-loss microwire-like mode with electromagnetic energy confined to the ZnO microwire core (Fig. 4(a) and (d)). Conversely, a smaller-width microwire results in a very weak localization parallel to the metal surface and suffers a loss comparable to that of uncoupled SPPs. Evidently, the gap provides the means to store electromagnetic energy, and leads to subwavelength confinement with low mode loss. The electric field distributed in the ultrasmall gap region demonstrates that the collective oscillation of the electrons in the metal film can be activated and surface plasmon wave can be spread along the axial direction at the interface between the metal and low dielectric layer. The mode characteristics of the hybrid plasmonic F–P microcavity calculated as shown in Fig. 3 is consistent with Fig. 4. When the width of the ZnO microwire with quadrate cross-section is large enough, the incident light energy can mainly be focused within the microwire. Here we define the gap region as the area of low-permittivity dielectrics directly beneath the microwire and above the metal. The strong energy confinement in the gap region occurs for two reasons. Firstly, it arises from the continuity of the displacement field at the material interfaces, which leads to a strong normal electric-field component in the gap. Secondly, in both uncoupled SPP and cylinder geometries, the electric-field components normal to the material interfaces are dominant, amplifying the first effect. In fact,

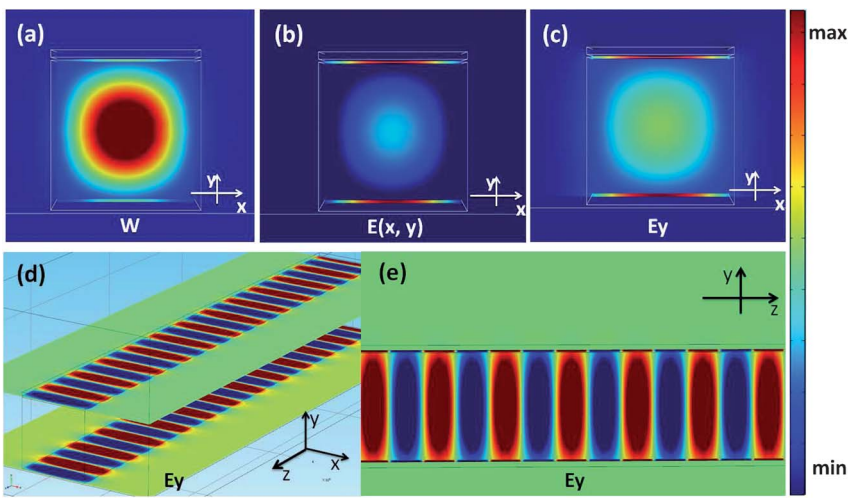

Fig. 3 The mode characteristics of the hybrid plasmonic Fabry–Perot microcavity: (a)–(c) normalized energy density **W**, **E**(**x**, **y**) and $\mathbf{E}_y$ distribution of the cross-section of the microcavity structure; (d) the y component of the electrical field distribution $\mathbf{E}_y$ along the z axis, which means that the surface plasmon wave excited at the interface between metal films and SiO_2 can be transmitted along the interface; (e) the y component of the electrical field distribution $\mathbf{E}_y$ along the y–z plane, when the excitation light source strikes at the cross-section of the microwire, the incident light spreads within the microwire.

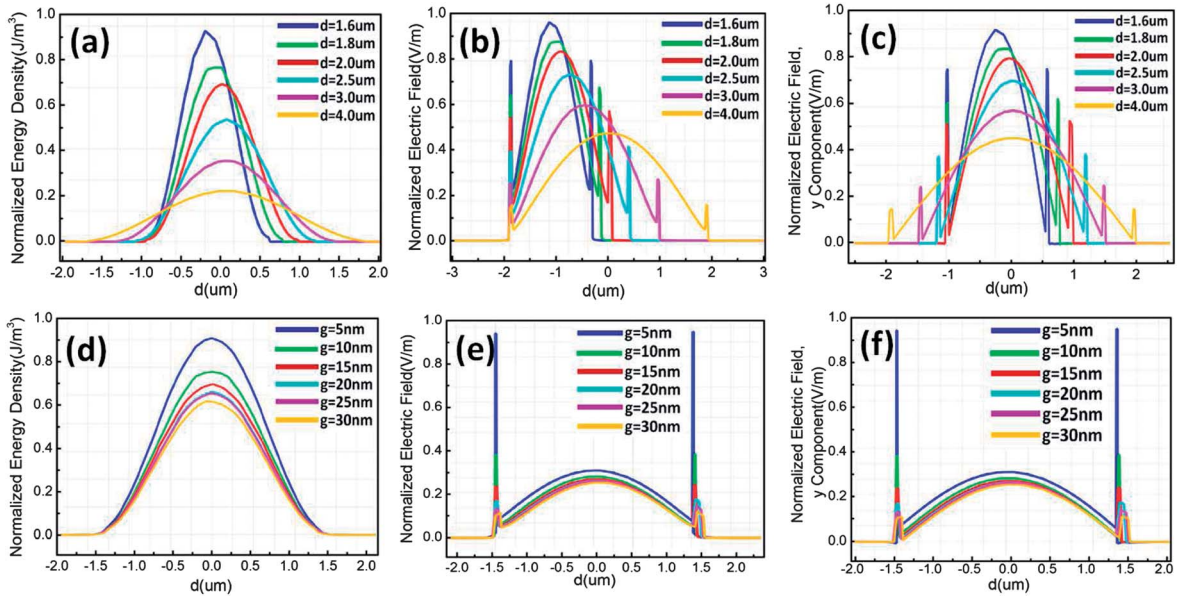

Fig. 4 Distribution of energy density **W**, electric field **E**(x, y) and the *y* component of electric field E_y of the cross-section of the ZnO microwire with the variables of the gap distance *g* and width of the ZnO microwire *d*: (a)–(c) demonstrate the energy density **W**, **E**(x, y) and E_y of the cross-section of the ZnO microcavity with *d* ranged from 1.6 μm to 4 μm respectively; (d)–(f) demonstrate the energy density **W**, **E**(x, y) and E_y of the cross-section of the ZnO microcavity with *g* ranged from 5 nm to 30 nm, respectively.

the dielectric discontinuity at the semiconductor-low dielectric material interface produces polarization charges that interact with the plasma oscillations of the metal-low dielectric material interface; that is, the gap region has an effective optical capacitance, similar to that of a closely spaced metallic wire and plane.[26,32,35]

Fig. 5(a) demonstrates that light waves that are transmitted oscillate back and forth inside the cavity. Fig. 5(b) shows the electric field distribution along the $x = 0$ of the quadrate cross-section of the microwire with the width of the ZnO microwire $d = 3$ μm and gap distance $g = 5$ nm. This special electric field distribution shows that part of the incident light energy is absorbed by the metal film; therefore, collective oscillation of the electrons and surface plasmon can be activated. When the photon momentum released by the ZnO microwire is consistent with the momentum of surface plasmon wave, surface plasmon resonance could be realized between the ZnO microwire mode and plasmonic F–P microcavity mode. Fig. 5(c) indicates that the images of each cross-section are stacked vertically next to a diagram of a vertical microwire to show the energy density **W** distribution from each corresponding vertical section. These images in particular demonstrate that the incident energy is mainly distributed in the ZnO microwire and gap with low dielectric material. The spaser could store energy, which may be used to stimulate collective oscillation of the electrons in the metal film and surface plasmon.

The three dimensional space structure of the hybrid plasmonic F–P microcavity has been simulated with variables, such as the width of the ZnO microwire with quadrate cross-section and the gap distance between metal films and the ZnO microwire. Detailed simulation results are shown in Fig. 3–5. The hybrid plasmonic F–P microcavity can support light transmission, collective oscillation of electrons, as well as surface plasmon resonance between between the ZnO microwire and plasmonic MIM homostructures. This new type of hybrid plasmonic microcavity can be used to realize many exciting applications in strong-coupling cavity quantum electrodynamics (QED), enhancement and suppression of spontaneous emission, such as microlasers, optomechanics, biological sensors, and SERS.

3. Experimental

ZnO microwires were synthesized *via* a traditional chemical vapor deposition method in a horizontal tube furnace. A mixture of ZnO and graphite powders with a definite weight ratio of 1 : 1 served as the reactive source. The silicon substrate with about 100 nm thick ZnO films deposited *via* a radio frequency magnetron sputtering method was laid above the source material with a vertical distance of 4 mm. The growth temperature was 1030 °C, and the furnace was heated to 1030 °C in 20 min from room temperature. After the reaction for 30 min, the furnace was cooled down to room temperature naturally. The microwires could be observed on the substrate and the inner surface of the boat. During the synthesis process, a constant flow of argon (99.99%) (100 standard cubic centimeters per minute) was introduced into the tube furnace using it as the protecting gas.

A ZnO microwire with quadrate cross-section is shown in Fig. 6(a) and (b), the width of ZnO microwires ranged from 1 μm to 7 μm, with its length at the centimeter level. In order to eliminate SPP scattering and to reduce metal loss, part of the ZnO microwire was selected to construct the hybrid plasmonic F–P microcavity. The experimental process of the hybrid

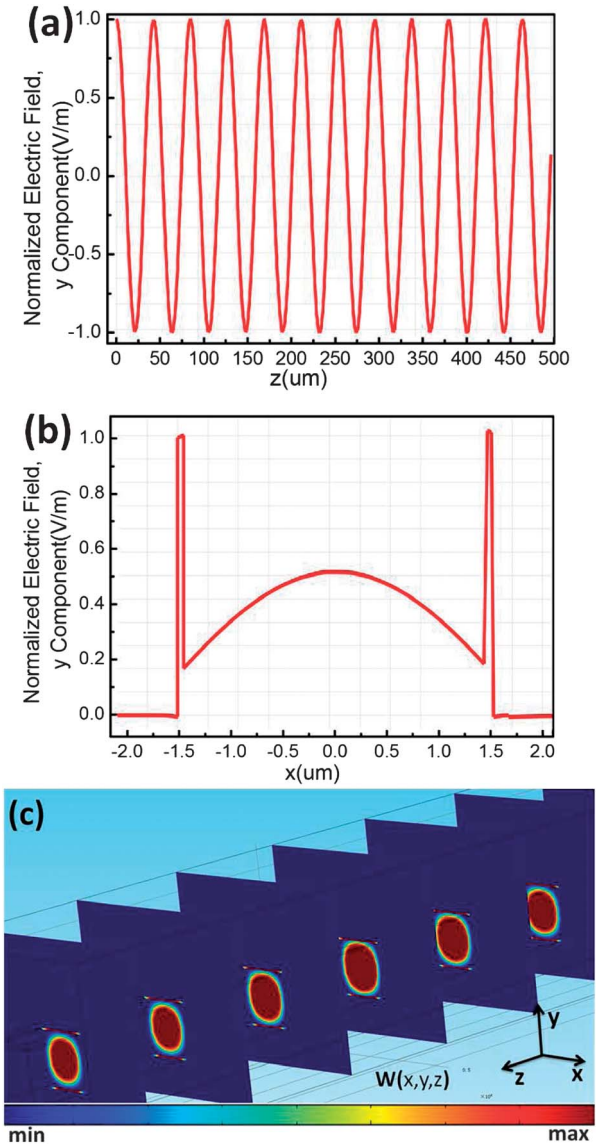

Fig. 5 Characteristics of the hybrid plasmonic F–P microcavity: (a) shows that the incident light can be transmitted along the axial direction of the ZnO microwire, with the length of the ZnO microwire denoted as $l = 500$ μm; (b) shows the electromagnetic field distribution along the $x = 0$ of the quadrate cross-section of the microwire with the width of the ZnO microwire $d = 3$ μm, and the gap distance $g = 5$ nm; (c) diagram of the hybrid plasmonic F–P microcavity with the ZnO vertical microwire with the corresponding energy density **W** distribution along the axis of the ZnO microwire.

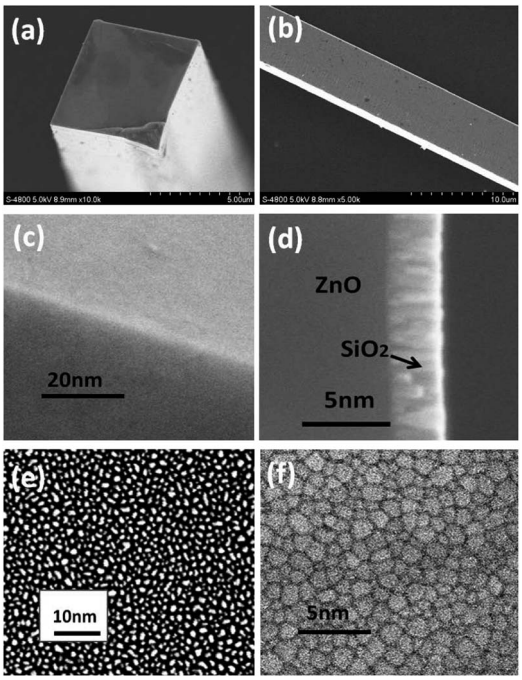

Fig. 6 SEM images of a single ZnO microwire on a silicon substrate: (a) shows the cross-section of the ZnO microwire; the width is about 4 μm; (b) a ZnO microwire on sapphire directed along the polar *c*-axis exhibiting a quadrilateral crystal symmetry, (c) smooth surface of the ZnO microwire indicates high quality. (d) SEM image of a SiO_2 thin film prepared on the surface of the ZnO microwire. (e) Surface texture images of the Ag film prepared on a SiO_2 thin film with 30 s sputtering time. (f) Shows surface texture images of the Ag film prepared on a SiO_2 thin film with 1 min sputtering time.

plasmonic Fabry–Perot microcavity is the preparation of a layer of silver film on the substrate firstly, and a layer of SiO_2 thin film preparation, using external force to press the ZnO microwire printed on the SiO_2 thin film, then preparation of a microwire above a layer of SiO_2, and finally the preparation of another layer of silver film. The time for evaporating Ag was about 30 s, 1 min, 2 min, and 4 min. Fig. 6(c) demonstrates the smooth surface of the ZnO microwire, which means that it is a high quality crystal. Fig. 6(d) shows the image of a SiO_2 film prepared on the surface of the ZnO microwire. Fig. 6(e) and (f) show the SEM image of the surface texture of the silver film with 30 s sputtering time and 1 min sputtering time, respectively. Especially for Fig. 6(f), long durations of evaporation of silver on the medium surface can form a layer of silver film. The preparation of the metal films and microcavity structures is carried out under vacuum conditions.

The morphology of the microwire was characterized by field emission scanning electron microscopy (FESEM). The photoluminescence (PL) measurement was carried out with a JY-630 micro-Raman spectrometer by using the 325 nm line of a He–Cd laser as the excitation source.[36]

4. Results and discussion

The laser character, as well as the relationship of the integrated emission intensities *versus* the excitation power density has been confirmed.[12] So much attention to the enhanced characteristics of the microcavity will mainly be paid to in this study. The PL spectrum of the ZnO microwire excited by using the He–Cd laser was analyzed at room temperature. In order to properly compare the PL peak intensities, we choose a single ZnO microwire with 5 sections, from point 1 to point 5, as shown in Fig. 7. A strong emission peak located at 380 nm could be observed, which corresponds to the near band edge emission of ZnO. Defect related visible emission is very low, suggesting that the ZnO microwire is of high crystal quality. Fig. 8 shows the PL

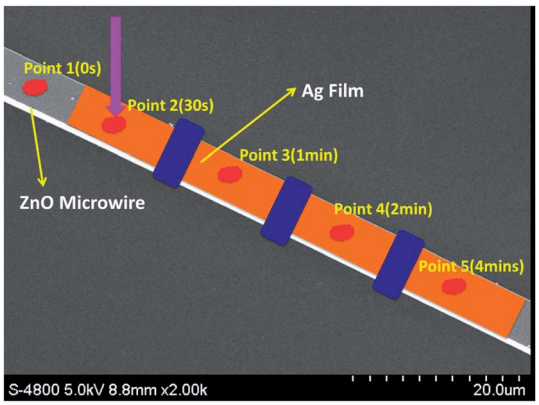

Fig. 7 The optical image of the plasmonic Fabry–Perot microcavity consisting of ZnO MWs covered with double Ag films, point 1 demonstrates the bare ZnO microwire section, point 2 to point 5 illustrate 30 s, 1 min, 2 min, and 4 min sputtering times, respectively.

spectra of a typical hybrid plasmonic F–P microcavity based on the Ag film coated ZnO microwire and a bare ZnO microwire at room temperature. The PL peak of the hybrid structure does almost not shift with respect to that of the bare ZnO microwire, and the strongest PL peak intensities from the hybrid structure are approximately 100 times larger than those of the bare ZnO microwire. The PL intensity of the hybrid structures strongly depends on the thickness of the Ag film layer, as well as the distance between the ZnO microwire and the Ag films. These results demonstrate that the PL enhancement of the hybrid plasmonic F–P microcavity originated from two reasons: firstly, photons can be oscillated repeatedly in a microcavity body and is absorbed by the ZnO microwire, when light hits the interface, the metal film can enhance the reflection of light, so as to realize the enhancement of optical oscillation; secondly, when light hits the interface between metal films and low dielectric medium, surface plasmon polaritons and collective oscillations of free electrons can be activated. Coated with metal films on the surface of the ZnO microwire, the emitted photons from ZnO with the in-plane momentum can excite the surface plasmons of metal medium. The surface plasmons can convert into photons and be captured by the measurement system, which leads to the PL intensity enhancement. Therefore, from the perspective of interaction between hybrid modes, the F–P microcavity based on the hybrid plasmonic waveguide can support the surface plasmon wave long-range transmission and enhance reflection inside the microcavity. The enhancement PL peak intensity from the hybrid structure attributes to the coupling coherent interaction between plasmonic microcavity modes and the ZnO microwire mode.

To confirm the enhancement of PL intensity derived from the hybrid plasmonic F–P microcavity, two kinds of structures using Ag and Au films were constructed as shown in the inset of Fig. 9. MIM homostructures that consisted of double gold films were investigated and a ten times PL enhancement was observed, as shown in Fig. 9(a), the corresponding model structure is shown in the inset of Fig. 9(a). Then we just prepared a single silver thin film, and the model structure shown in the inset of Fig. 9(b). The hybrid structure results in a four times PL enhancement. Metals as candidates for plasmonic materials have been investigated, and it is found that compared with gold, silver is more suitable for UV bands.[39] The PL enhancement of MIM homostructures consisted of double gold films is indeed due to the hybrid plasmonic F–P microcavity, meanwhile the PL enhancement of the hybrid waveguide that consisted of a single silver film is mainly derived from silver surface plasmons.

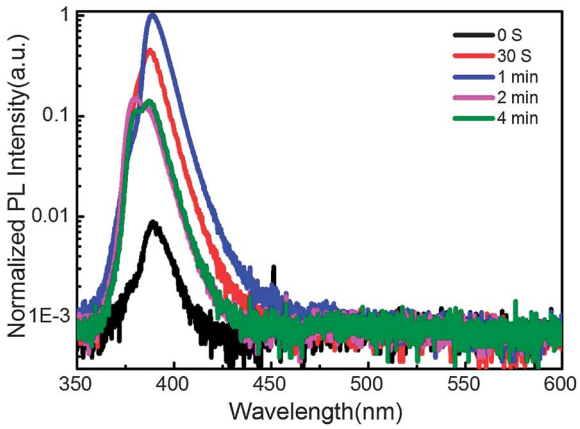

Fig. 8 PL spectra of ZnO MWs excited at point 1 to point 5, similar to those shown in Fig. 7 with different sputtering times, 0 s, 30 s, 1 min, 2 min, and 4 min, respectively.

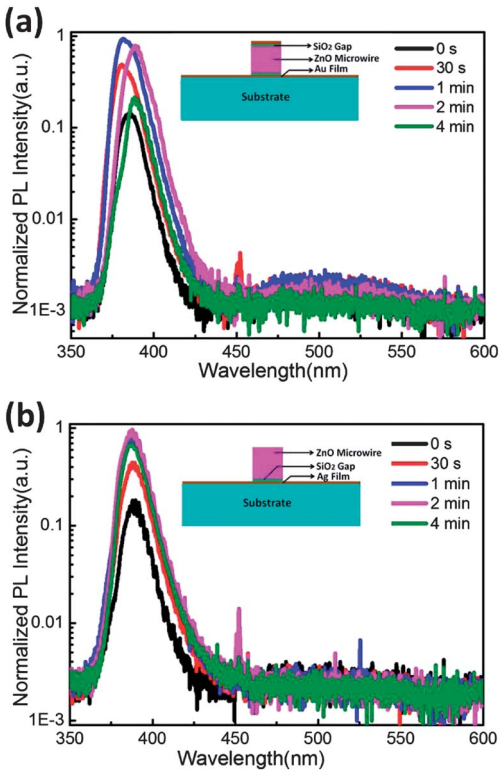

Fig. 9 Normalized PL spectra of the nanostructure: (a) inset of the graph is the mode of the hybrid plasmonic microcavity; (b) inset of the graph is the mode of the hybrid plasmonic waveguide.

The mode characteristics of the hybrid plasmonic F–P microcavity and more than two orders of magnitude of the ultraviolet photoluminescence intensities from the hybrid plasmonic F–P microcavity of the Ag/ZnO microwire is stronger than a bare ZnO microwire have been demonstrated. The enhancement is due to the strong coupling between the microcylinder waveguide mode and the surface plasmon mode supported by the MIM homostructures. The mechanism of this enhanced ultraviolet photoluminescence is analyzed based on the plasmonic F–P microcavity and the coupled mode theory. In addition, we have demonstrated that the ultraviolet photoluminescence applied to a single dielectric microscale cylinder in the hybrid plasmonic waveguide is much stronger than that in the photonic waveguide. So choosing a suitable metal material to construct a hybrid plasmonic F–P microcavity based on a ZnO microwire with quadrate cross-section is the essential reason to improve the luminescence enhancement. The enhancement mechanism derived from the hybrid plasmon F–P microcavity provides an approach to further study ZnO laser action and to improve the laser output power. The strongly enhanced ultraviolet photoluminescence enables the applications of luminescence at the nanometer scale, opening a new realm for many exciting applications.[25,40]

5. Conclusion

In summary, we have built a kind of plasmonic F–P microcavity consisting of a plasmonic MIM homostructure and a ZnO microwire with quadrate cross-section. This type of microcavity structure can support subwavelength confinement and long range propagation, attributed to the coupling between the photonic microcavity mode and the hybrid plasmonic cavity mode. ZnO microwires with quadrate cross-section have also been synthesized, and the PL properties of the hybrid plasmonic F–P microcavity were studied; a photoluminescence enhancement of 2 orders of magnitude was achieved. The enhancement is derived from the resonant coupling excitation of hybrid plasmonic waveguide mode and the ZnO microwire F–P cavity mode. This study indicates that the plasmonic F–P microcavity with quadrilateral ZnO microwires has the potential to be applied in microlaser diodes.

Acknowledgements

This work is supported by the National Basic Research Program of China (973 Program) (nos. 2011CB302006 and 2011CB302004), the National Natural Science Foundation of China (nos. 10974197, 11174273, 11104265, and 21101146), and the 100 Talents Program of the Chinese Academy of Sciences.

References

1 K. J. Vahala, *Nature*, 2003, **424**, 839–846.
2 E. Schubert, N. Hunt, M. Micovic, R. Malik, D. Sivco, A. Cho and G. Zydzik, *Science*, 1994, **265**, 943–945.
3 M. H. Huang, S. Mao, H. Feick, H. Yan, Y. Wu, H. Kind, E. Weber, R. Russo and P. Yang, *Science*, 2001, **292**, 1897–1899.
4 Y.-Y. Lai, Y.-P. Lan and T.-C. Lu, *Light: Sci. Appl.*, 2013, **2**, e76.
5 B. Min, E. Ostby, V. Sorger, E. Ulin-Avila, L. Yang, X. Zhang and K. Vahala, *Nature*, 2009, **457**, 455–458.
6 S. Chu, G. Wang, W. Zhou, Y. Lin, L. Chernyak, J. Zhao, J. Kong, L. Li, J. Ren and J. Liu, *Nat. Nanotechnol.*, 2011, **6**, 506–510.
7 G. Reguera, K. D. McCarthy, T. Mehta, J. S. Nicoll, M. T. Tuominen and D. R. Lovley, *Nature*, 2005, **435**, 1098–1101.
8 C. Dang, J. Lee, Y. Zhang, J. Han, C. Breen, J. S. Steckel, S. Coe-Sullivan and A. Nurmikko, *Adv. Mater.*, 2012, **24**, 5915–5918.
9 X.-Y. Liu, C.-X. Shan, S.-P. Wang, Z.-Z. Zhang and D.-Z. Shen, *Nanoscale*, 2012, **4**, 2843–2846.
10 H. Zhu, C.-X. Shan, J.-Y. Zhang, Z.-Z. Zhang, B.-H. Li, D.-X. Zhao, B. Yao, D.-Z. Shen, X.-W. Fan, Z.-K. Tang, *et al.*, *Adv. Mater.*, 2010, **22**, 1877–1881.
11 S. Bize, *Nat. Photonics*, 2012, **6**, 638–639.
12 M. Ding, D. Zhao, B. Yao, Z. Guo, L. Zhang, D. Shen, *et al.*, *Opt. Express*, 2012, **20**, 13657–13662.
13 J. Dai, C. X. Xu and X. W. Sun, *Adv. Mater.*, 2011, **23**, 4115–4119.
14 Z. Tang, G. K. Wong, P. Yu, M. Kawasaki, A. Ohtomo, H. Koinuma and Y. Segawa, *Appl. Phys. Lett.*, 1998, **72**, 3270.
15 M. A. M. Versteegh, D. Vanmaekelbergh and J. I. Dijkhuis, *Phys. Rev. Lett.*, 2012, **108**, 157402.
16 Y. Liu, H. Dong, S. Sun, W. Liu, J. Zhan, Z. Chen, J. Wang and L. Zhang, *Nanoscale*, 2013, **5**, 4123–4128.
17 D. Vanmaekelbergh and L. K. van Vugt, *Nanoscale*, 2011, **3**, 2783–2800.
18 D. J. Gargas, M. C. Moore, A. Ni, S.-W. Chang, Z. Zhang, S.-L. Chuang and P. Yang, *ACS Nano*, 2010, **4**, 3270–3276.
19 K. Ding and C. Ning, *Light: Sci. Appl.*, 2012, **1**, e20.
20 P. Berini and I. De Leon, *Nat. Photonics*, 2011, **6**, 16–24.
21 V. J. Sorger, R. F. Oulton, J. Yao, G. Bartal and X. Zhang, *Nano Lett.*, 2009, **9**, 3489–3493.
22 R. Ameling and H. Giessen, *Nano Lett.*, 2010, **10**, 4394–4398.
23 W. Cai, J. S. White and M. L. Brongersma, *Nano Lett.*, 2009, **9**, 4403–4411.
24 Y.-J. Lu, J. Kim, H.-Y. Chen, C. Wu, N. Dabidian, C. E. Sanders, C.-Y. Wang, M.-Y. Lu, B.-H. Li, X. Qiu, *et al.*, *Science*, 2012, **337**, 450–453.
25 Y.-K. Liu, S.-C. Wang, Y.-Y. Li, L.-Y. Song, X.-S. Xie, M.-N. Feng, Z.-M. Xiao, S.-Z. Deng, J.-Y. Zhou, J.-T. Li, *et al.*, *Light: Sci. Appl.*, 2013, **2**, e52.
26 R. F. Oulton, V. J. Sorger, D. Genov, D. Pile and X. Zhang, *Nat. Photonics*, 2008, **2**, 496–500.
27 R. F. Oulton, V. J. Sorger, T. Zentgraf, R.-M. Ma, C. Gladden, L. Dai, G. Bartal and X. Zhang, *Nature*, 2009, **461**, 629–632.
28 V. I. Belotelov, A. N. Kalish, A. K. Zvezdin, A. V. Gopal and A. S. Vengurlekar, *J. Opt. Soc. Am. B*, 2012, **29**, 294–299.
29 S. Chen, G. Li, D. Lei and C. Kok-wai, *Nanoscale*, 2013, **5**, 9129–9133.
30 S.-W. Chang, T.-R. Lin and S. L. Chuang, *Opt. Express*, 2010, **18**, 15039–15053.

31 X. Li, J. D. Budai, F. Liu, J. Y. Howe, J. Zhang, X.-J. Wang, Z. Gu, C. Sun, R. S. Meltzer and Z. Pan, *Light: Sci. Appl.*, 2013, **2**, e50.
32 H. Jiang, C. Liu, P. Wang, D. Zhang, Y. Lu and H. Ming, *Opt. Express*, 2013, **21**, 4752–4757.
33 X. Yang, A. Ishikawa, X. Yin and X. Zhang, *ACS Nano*, 2011, **5**, 2831–2838.
34 V. J. Sorger, N. Pholchai, E. Cubukcu, R. F. Oulton, P. Kolchin, C. Borschel, M. Gnauck, C. Ronning and X. Zhang, *Nano Lett.*, 2011, **11**, 4907–4911.
35 R.-M. Ma, R. F. Oulton, V. J. Sorger, G. Bartal and X. Zhang, *Nat. Mater.*, 2010, **10**, 110–113.
36 R. Liu, X. Fu, J. Meng, Y.-Q. Bie, D. Yu and Z.-M. Liao, *Nanoscale*, 2013, **5**, 5294–5298.
37 M. Noginov, G. Zhu, A. Belgrave, R. Bakker, V. Shalaev, E. Narimanov, S. Stout, E. Herz, T. Suteewong and U. Wiesner, *Nature*, 2009, **460**, 1110–1112.
38 D. J. Bergman and M. I. Stockman, *Phys. Rev. Lett.*, 2003, **90**, 027402.
39 P. R. West, S. Ishii, G. V. Naik, N. K. Emani, V. M. Shalaev and A. Boltasseva, *Laser Photonics Rev.*, 2010, **4**, 795–808.
40 E. Matioli, S. Brinkley, K. M. Kelchner, Y.-L. Hu, S. Nakamura, S. DenBaars, J. Speck and C. Weisbuch, *Light: Sci. Appl.*, 2012, **1**, e22.